This is an *Accepted Manuscript*, which has been through the Royal Society of Chemistry peer review process and has been accepted for publication.

Accepted Manuscripts are published online shortly after acceptance, before technical editing, formatting and proof reading. Using this free service, authors can make their results available to the community, in citable form, before we publish the edited article. We will replace this *Accepted Manuscript* with the edited and formatted *Advance Article* as soon as it is available.

You can find more information about *Accepted Manuscripts* in the **Information for Authors**.
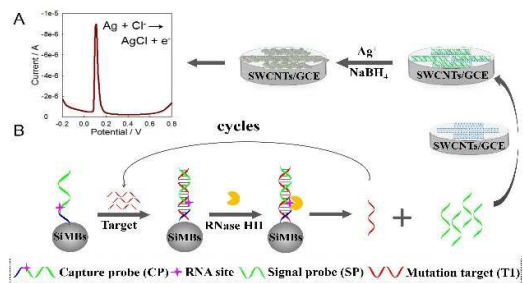
In this communication, we proposed an electrochemical sensing strategy for T2DM-related SNP detection *via* DNA-mediated AgNPs growth on SWCNTs-modified electrode.

Journal Name

COMMUNICATION

Electrochemical Detection of Type 2 Diabetes Mellitus-Related SNP *via* DNA-Mediated Growth of Silver Nanoparticles on   Single Walled Carbon Nanotubes

Jia Tao,[a,c] Peng Zhao,[b] Jing Zheng,[b,*] Cuichen Wu,[b] Muling Shi,[b] Jishan Li,[b] Yinhui Li[b] and Ronghua Yang [a,b,*]

Herein, we proposed a new electrochemical sensing strategy for T2DM-related SNP detection *via* DNA-mediated growth of AgNPs on SWCNTs-modified electrode. Coupling with RNase HII enzyme assisted amplification, this approach could realize T2DM-related SNP assay and be applied in crude extracts of carcinoma pancreatic β-cell lines.

Type 2 diabetes mellitus (T2DM) which refers to a series of disparate metabolic diseases, can cause potential complications including heart disease, stroke and kidney damage.[1-3] Efforts made in defining the molecular mechanism of T2DM have identified that mitochondrial DNA (mtDNA) mutations are strongly related to T2DM, with the most common single nucleotide polymorphism (SNP) being the A3243G mutation in mtDNA-encoded tRNA[Leu(UUR)] gene.[4-6] Therefore, the SNP detection of mtDNA is significant for early diagnosis and clinical treatment of T2DM. Electrochemical strategy has gained comprehensive interests because it allows the development of sensitive and accurate, yet inexpensive, real-time and robust gene-sensing platforms.[7] In spite of considerable progress, the conventional electrochemical methods commonly utilize small electroactive molecules to generate measurable signal, and thus false positive or high background noise caused by the nonspecific adsorption still remains a challenge.[8]

Silver nanoparticles (AgNPs) have been proved to be an excellent electrochemical tag due to their lower oxidation potential with a relatively sharp peak, which is favorable to obviate the interference of reducing species and thus improve detection precision and sensitivity.[9] However, the conjugation of AgNPs onto the electrode surface usually lead to high cost and tedious operation. Biomineralization, which refers to the biologically-controlled formation of mineral deposits, can serve as a powerful strategy.[10-12] DNA has been used as a controllable, and adaptable biomineralization template whose physical properties can be explored to synthetize AgNPs.[13-14] Inspired by the excellent performance of AgNPs in electrochemical sensing

and as a continuation of our studies on the DNA-mediated growth of AgNPs on the surface of single walled carbon nanotubes (SWCNTs) which are suitable for accelerating the transmitting rate of electrons,[15] herein, we are interested in whether this *in situ* growth of AgNPs-based strategy could be explored as an effective and simple electrochemical assay in the determination of T2DM-related SNP. As shown in Scheme 1A, we found this DNA-mediated AgNPs yielding on the surface of SWCNTs-absorbed glass carbon electrode (SWCNTs/GCE) demonstrated an excellent single strand DNA (ssDNA) concentration-dependent electrochemical signal.
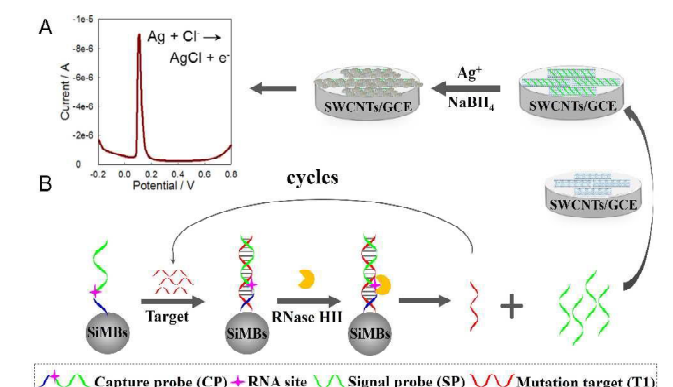
Scheme 1. Design scheme of (A) DNA-mediated growth of AgNPs on SWCNTs/GCE and (B) coupling with RNase HII for amplified electrochemical detection of T2DM-related single-nucleotide polymorphisms.

Inspired by this, we proposed a new label-free electrochemical strategy for T2DM-related SNP detection *via* DNA-mediated growth of AgNPs on SWCNTs/GCE surface coupling with   RNase HII-assisted amplification. The substitution (A>G) at nucleotide position (np) 8344 in mtDNA was selected as a model target.[16] The mechanism of RNase HII-amplified detection of T2DM-related mutation mtDNA was shown in Scheme 1B, the capture probe (CP) was conjugated

onto silica microbead (SiMB) surface through streptavidin-biotin interaction. It is worth noting that a single ribonucleotide was embedded in the middle of the capture probe. Upon target binding, the duplex fragments of 5'-DNA-RNA-DNA-3'/3'-DNA-5' were recognized by RNase HII, which can catalyze the hydrolysis of phosphodiester bond 5' to the ribonucleotide at the DNA-RNA junction.[17-18] After nicking, the hybridization between capture probe and target became less stable, and target fragment dissociated from the quadripartite complex. The released target strand could bind with another CP while numerous ssDNA were generated as the signal probes (SPs). Consequently, the SPs could serve as the templates for *in situ* growth of AgNPs after SiMBs were separated from the solution by centrifugation.

To fabricate high sensitive electrochemical active substrates, ssDNA-mediated SWCNTs@AgNPs were firstly proceeded using in situ Ag+ attachment and seeded growth methods. The sequence of ssDNA was the same as the SP (see in Table S1, ESI†). Transmission electron microscope (TEM) image of the synthesized SWCNTs@AgNPs revealed that AgNPs were densely decorated on the surface of ssDNA wrapped-SWCNTs (SWCNTs/ssDNA) after seeded growth, as shown in Fig. S1 (ESI†). Then, the distribution of particle size was analyzed. The minimal size was 5.6 nm while the maximum size was 21.5 nm. The average size was about 10 ± 0.9 nm, which was consistent to the previous report using similar methods.[12] We next used atomic force microscope (AFM) to characterize the morphology of the AgNPs-decorated SWCNTs, which exhibited that the as- synthesized AgNPs linearly distributed and the average height was about 8 nm, higher than the bare SWCNTs alone (Fig. S2, ESI†). All these collective results demonstrated that ssDNA had actually assisted in serving as "nanoscaffold" for Ag+, subsequently, formed DNA-mediated SWCNTs@AgNPs upon reduction, which was the foundation for the following design of our label free electrochemical sensor.

After demonstration of the *in situ* growth of AgNPs on SWCNTs, the DNA-templated SWCNTs@AgNPs-based electrode was then fabricated. Since SWCNTs have a strong binding force with GCE through van der Waals interactions, DNA can thus be adsorbed on SWCNTs-decorated GCE surface *via* π-π interaction. We next characterized each step of fabricating SWCNTs@AgNPs/GCE by electrochemical impedance spectroscopy (EIS, Fig. 1A). The resistance of bare GCE was about 500 Ω (curve a), while the value was sharply decreased to about 0 Ω (curve b) after modification of SWCNTs (SWCNTs/GCE) which was suitable for accelerating the transmitting rate of electrons. The DNA/SWCNTs/GCE exhibited much larger electron transfer resistance (Ret=~850 Ω, curve c), which can be attributed to the stronger backbone of DNA toward $Fe(CN)_6^{3-/4-}$. Then, AgNO3 was dropped onto the surface of DNA/SWCNTs/GCE to form DNA/Ag+ complex. After rinsing thoroughly with certain amount of water for three times, the SWCNTs@AgNPs/GCE was acquired upon NaBH4 addition. Subsequently, the decreased Ret in EIS spectra indicated that the complete biometallization of DNA has greatly enhanced the conductance property of DNA (curve d).

Correspondingly, as shown in Fig. 1B, bare GCE presented no differential pulse voltammetry (DPV) current (curve a) while similar results could be obtained after SWCNTs addition (SWNCTs/GCE, curve b) and subsequent DNA addition (DNA/SWCNTs/GCE, curve c) under DPV scan. It was noteworthy that a distinct sharp oxidation peak current (about 0.16 V) could be observed after *in situ* growth of AgNPs (curve d).Also, the oxidation potential was similar to the reported results,[9] which was certified as the solid state transforming from Ag to the AgCl on the surface of SWCNTs/GCE (Fig.S3, ESI†). This process indicated that the electron transferred from AgNPs to the electrode surface, which could be summarized by the next equation:

$$AgNPs(solid) + Cl^-(solution) \rightarrow AgCl(solid) + e^-$$

These results indicated that this DNA-mediated *in situ* growth of AgNPs was an attractive approach for the self-assembly of nanoelectronics. Then, the correlation between peak current intensity of SWCNTs@AgNPs/GCE and ssDNA concentration was investigated. Fig. S4 (ESI†) revealed that the DPV signal increased dramatically as functions of different concentrations of ssDNA under optimal conditions (optimized concentration of AgNO3, NaBH4 were 20 μM and 1 mM, the growth time was 20 min, as shown in Fig. S5, S6 and S7, ESI†). The DPV signal linearly increased with the concentration of ssDNA ranging from 5 to 50 nM (Fig. 1C). The limit of detection, based on $3\sigma_b$/slope, where σ_b was the standard deviation of blank samples, was 3 nM. This result could also be improved by rational introduction of signal amplification strategy.
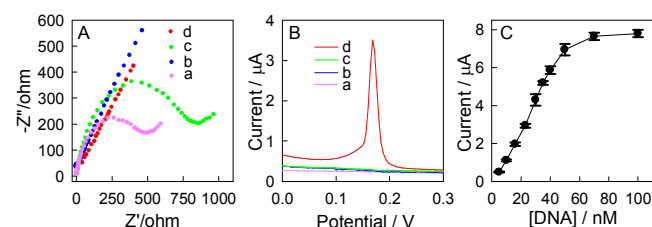
Fig. 1 (A) EIS and (B) DPV scan of bare GCE(a), SWCNTs/GCE(b), DNA/SWCNTs/GCE(c) and SWCNTs@AgNPs/GCE(d). [ssDNA]=30 nM. (C) The relationship between peak current intensity of SWCNTs@AgNPs/GCE and ssDNA concentration (5 nM-50 nM). [SWCNTs]=0.1 mg/mL, [AgNO3]=20 μM, [NaBH4]=1 mM. The concentration of SWCNTs is excessive.

The adenine for guanine substitution (A→G) at nucleotide position (np) 8344, which lies in the human mtDNA control region for replication and transcription, has been reported to be associated with insulin resistance and T2DM in Asians.[12] Therefore, the discrimination of A8344G polymorphism is of great significance to cast light on its association with T2DM and can be used as a reference for the prediction of the risk for T2DM. In our design, two 33 bp oligonucleotide sequences originated from human mtDNA, T1 and T2, were chose as a mutation and wild type target, respectively (sequences was shown in Table S1, ESI†). Polyacrylamide gel electrophoresis (PAGE) was firstly performed to investigate the RNase HII-catalyzed cleavage. As shown in Fig. S8 (ESI†), after incubated CP/T1 or CP/T2 hybrid duplex with RNase HII, the former

complex could be cleaved into a short length strand. A faint band was ascribed to the hydrolysis product while the CP/T2 complex stayed stable and remained intact, confirming that RNase HII could recognize and catalyze the hydrolysis of phosphodiester bond 5' to the ribonucleotide at the perfect DNA-RNA junction.

We then investigated the feasibility of our constructed DNA-templated AgNPs-based electrochemical sensor for the detection of T2DM-related SNP. As shown in Fig. 2, in the absence of target DNA T1, no peak current under DPV scan could be observed which was mainly due to the DNA template lacking (curve a). Upon addition of T1 to the mixture, the CP/T1 binding resulted in the formation of a double strand and remarkable DPV signal enhancement (about 6.45 μA) was acquired with the aid of RNase HII (curve b), suggesting that a large amount of SP were generated by the cleavage of RNase HII, which could serve as templates for the *in situ* growth of AgNPs on the surface of SWNCT/GCE. However, negligible electrochemical signal was observed in the presence of T2. This was mainly because that the RNA base embedded in CP couldn't be nicked by RNase HII without formation of perfect DNA-RNA junction (curve c). On the contrary, the control experiments demonstrated that no evident DPV signal could be observed without RNase HII addition even in the presence of T1 or T2 (curve d and curve e), further indicating that RNase HII indeed play an important role in amplified detection. All these results imply that this new electrochemical sensor coupling with RNase HII-assisted amplification has a potential for sensing the mutation target DNA.
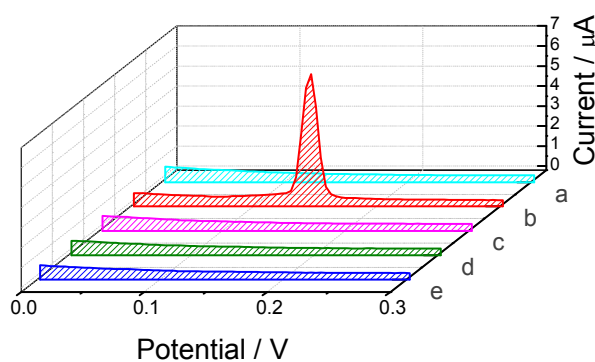
Fig. 2 DPV curves obtained from SWCNTs/GCE under different conditions. The data correspond to the DPV signal recorded in the absence of T1 or T2 (curve a) and presence of 10 nM T1 (curve b) and T2 (curve c). Curve d and e were obtained without the use of RNase HII in the presence of T1 (d) and T2 (e). [SWCNTs]=0.1 mg/mL, [AgNO₃]=20 μM, [NaBH₄]=1 mM. [SiMBs]=0.1 mg/mL, [CP]=50 nM, [RNase HII]=0.1 U/μL.

The reaction time and the concentration of RNase HII used in our design were then optimized for further quantitative analysis of target mutation mtDNA. In consideration of the balance between complete cleavage by RNase HII, the moderate concentration of RNase HII (0.1 U/μL) and 60 min reaction time were chosen in the subsequent experiments (Fig. S9, ESI†). As shown in Fig. 3A, the DPV intensity increased dramatically with the increasing concentration of T1 under

optimal conditions, suggesting that RNase HII could successfully induce the cleavage of CP, meanwhile, the as-generated ssDNA-mediated AgNPs could serve as an effective electrochemical substrate for DNA detection (Fig. 3B). The plot of DPV intensity as the function of T1 concentration demonstrated a good linearity ranging from 10 pM to 10 nM with a detection limit of 3 pM, which is much lower than the reported similar work and could directly be used to detect genomic DNA.[19-20] Next, we have carefully examined the reproducibility for this proposed T2DM-related SNP detection. The experiments results revealed that SNP detection of 1 nM and 10 nM mutation target DNA showed an intra-assay RSD of 3.5% and 4.1% with five determinations, respectively. When the sensor was not in use, it was stored in air condition at room temperature and measured 100 mM PBS (pH 7.5) every day. No obvious change in the DPV intensity was observed after storage for at least 1 week (data not shown). All these results indicated the excellent reproducibility of the proposed sensor.
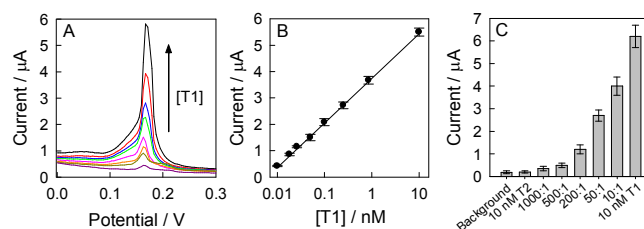
Fig. 3 (A) DPV curves of SWCNTs@AgNPs/GCE upon addition of different concentrations of T1. (B) The relationship between peak current intensity of SWCNTs@AgNPs/GCE and T1 concentration (10 pM-10 nM). (C) Response to none or different fractions of mutant target T1 in the mixture of T1 and T2, the total target concentration (T1 + T2) is 10 nM. [SWCNTs]=0.1 mg/mL, [AgNO₃]=20 μM, [NaBH₄]=1 mM. [SiMBs]=0.1 mg/mL, [CP]=50 nM, [RNase HII]=0.1 U/μL.

To further evaluate the specificity of our assay, we mixed T1 and T2 together in a total concentration of 10 nM at different molar ratios of 1000:1, 500:1, 200:1, 50:1 and 10:1 (Fig. 3C). In the control assay, no peak current was obtained upon T2 addition. However, in the presence of T1, even under the ratio value of T2 to T1 is 1000:1 (only 10 pM T1 in the mixture), the peak current still demonstrated a significant increase and higher than that of the control experiment using 10 nM T2. This result demonstrated the extraordinary capability of our strategy in the detection of a low-abundance mutation with a large quantity of the wild-types. The capability, along with its high sensitivity and simplicity, granted the assay a great potential in the clinical applications.

Then, we conducted the quantitative analysis of the mutation amount of T1 in the presence of 10 nM wild-type DNA T2. As was shown in Fig. S10, in the presence of wild-type DNA, the solid-state electrochemical signal also has a linear relationship with the concentration of T1 (10 pM to 10 nM), and the calculated limit of detection (LOD) was 5 pM. We can see that from Fig. S10, even the concentration of T1 was lower as 1/1000 of the T2, the sensor could output obvious signal. Thus, we conclude that this proposed method could be used to quantify the mutation amount in samples which have both mutated and wild-type DNA. Next, to investigate the interfering effects of sample matrix components on the electrochemical signal of our design, the sensing system was further applied for the detection of T1 in the complex systems including cell

media. As shown in Table S2, the results demonstrated that this strategy holds the potential to be applied to real sample.

Finally, this assay was performed on the crude extracts of carcinoma pancreatic β-cell lines from diabetes patients to prove the reliability of proposed method (Fig. S11, ESI†). This assay was applied to samples with the T1, T2 and crude extracts of carcinoma pancreatic β-cell lines from diabetes patients (1-10). For comparison, mtDNA from different samples (1-10) were extracted using tissue mitochondria isolation kit and DNA extraction kit, and their PCR products were sent to Sangon Biotech for Sanger sequencing services. The results of 10 cases had a good correlation to the Sanger sequencing results (Fig. S12, ESI†), indicating the applicability of this PCR-free approach in clinical diagnosis.

Conclusions

In summary, we proposed a new electrochemical sensing strategy for T2DM-related SNP detection *via* DNA-mediated growth of AgNPs on SWCNTs-modified electrode. The recognition of mutation target DNA could produce numerous ssDNA after hybridized with capture probe and hydrolyzed by RNase HII. The released ssDNA then served as the template for the *in situ* growth of AgNPs, whose solid-state electrochemical signal has a linear relationship to the quantity of target DNA. Our results demonstrated that this approach achieved a low detection limit of 3 pM for target DNA and also be successfully applied in crude extracts of carcinoma pancreatic β-cell lines from diabetes patients. The entire process is inexpensive and simple to prepare, and neither complicated sophisticated instruments are necessary. Combining these unique properties, we expect this approach will find its wide applications in T2DM for fundamental research, genomic research and clinical diagnostics.

Notes and references

*School of Chemistry and Biological Engineering, Changsha University of Science and Technology, Changsha, 410004, China; *State Key Laboratory of Chemo/Biosensing and Chemometrics, College of Chemistry and Chemical Engineering, Hunan University. Changsha, 410082, China; *College of Chemical Science and Engineering, South China University of Technology, Guangzhou, 510641, China.
E-mail: zhengjing2013@hnu.edu.cn, Yangrh@pku.ed.cn,*

Electronic Supplementary Information (ESI) available: More experimental details and spectroscopic data as noted in text.

1   C. J. Nolan, P. Damm, M. Prentki, *The Lancet*, 2011, **378**, 169.
2   M. L. Shi, J. Zheng, Y. J. Tan, G. X. Tan, J. S. Li, Y. H. Li, X. Li, Z. G. Zhou, R. H. Yang, *Anal. Chem.*, 2015, **87**, 2734.
3   L. Pasternak, E. Meltzer-Mats, G. Babai-Shani, G. Cohen, O. Viskind, J. Eckel, E. Cerasi, S. Sasson, A. Gruzman, *Chem. Commun.*, 2014, **50**, 11222.
4   B. B. Lowell, G. L. Shulman, *Science*, 2005, **307**, 384.
5   J. Van den Ouweland, H. Lemkes, W. Ruitenbeek, L. Sandkuijl, M. De Vijlder, P. Struyvenberg, J. Maassen, *Nat. Genet.*, 1992, **1**, 368.
6   A. H. V. Schapira, *The Lancet*, 2012, **379**, 1825.
7   B. J. Privett, J. H. Shin, M. H. Schoenfisch, *Anal. Chem.*, 2010, **82**, 4723.
8   X. B. Yin, *Trends Anal. Chem.*, 2012, **33**, 81.
9   D. J. Lin, J. Wu, M. Wang, F. Yan, H. X. Ju, *Anal. Chem.* 2012, **84**, 3662.
10   J. Zhang, B. P. Ting, N. P. Jana, Z. Q. Gao, J. Y. Ying, *Small*, 2009, **5**, 1414.
11   Y. Tao, E. G. Ju, J. S. Ren, X. G. Qu, *Chem. Commun.*, 2013, **49**, 9791.
12   X. Zhou, S. J. Xia, Z. Q. Lu, Y. Tian, Y. S. Yan, J. Zhu, *J. Am. Chem. Soc.*, 2010, **132**, 6932.
13   L. Wu, J. S. Wang, J. S. Ren, X. G. Qu, *Adv. Funct. Mater.*, 2014, **24**, 2727.
14   J. Wang, D. Xu, R. Polsky, *J. Am. Chem. Soc.*, 2002, **124**, 4208.
15   J. Zheng, J. H. Bai, Q. F. Zhou, J. S. Li, Y. H. Li, J. F. Yang, R. H. Yang, *Chem. Comm.*, 2015, **51**, 6552.
16   D. Sternberg, C. Danan, A. Lombès, P. Laforêt, E. Girodon, M. Goossens, S. Amselem, *Hum. Mol. Genet.*, 1998, **7**, 33.
17   Y. V. Gerasimova, S. Peck, D. M. Kolpashchikov, *Chem. Commun.*, 2010, **46**, 8761.
18   B. Rydberg, J. Game, *Proc. Natl. Acad. Sci. USA*, 2002, **99**, 16654.
19   H. G. Xu, W. Deng, F. J. Huang, S. Y. Xiao, G. Liu, H. J. Liang, *Chem. Commun.*, 2014, **50**, 14171.
20   H. Li, S. Y. Xiao, D. B. Yao, M. H. W. Lam, H. J. Liang, *Chem. Commun.*, 2015, **51**, 4670.